

# 60GHz resonant type $\text{LiNbO}_3$ light modulator

Satoshi Oikawa, Shinichi Shimotsu, and Tsutomu Saito

(Optoelectronics Research Group, New Technology Research Laboratory)

Masahide Sasaki, Tetsuya Kawanishi, and Masayuki Izutsu

(Communications Research Laboratory, Ministry of Posts and Telecommunications)

## ABSTRACT

We studied a  $\text{LiNbO}_3$  light modulator with a resonant type electrode operating at 60GHz band. In modulating 1.55 $\mu\text{m}$  wavelength light in on-off keying, the 3dB modulation band width was about 1GHz around 57.4GHz and the product between driving voltage and modulation length was 3.3  $\text{V}\pi\text{cm}$ . From this result, it will be possible to increase the modulation efficiency by improving the design of electrodes.

## 1. Introduction

The explosive boom of cellular phones and other means of mobile communications demands exploration of frequency resources for radio communications, especially in the millimeter band. However, high frequency transmission in the millimeter and other bands cannot cover long distances due to the large transmission losses, whether wired or radio. Studies have been made, as a result, to develop new technologies that combine broad-band optical fibers of low transmission losses for long distance transmission with radio communication.<sup>1)-4)</sup> Light modulated by radio signals travels through the optical fiber and is demodulated to electric signals at the other end. Here, the optical fiber is considered a transmission line of low-loss and broad-band radio communication. This will realize a new communication system that combines the distributability and mobility of radio communication and the broad-band capabilities and broad-band transferability of optical fiber communication. Such a system may be applied not only to cellular and other outdoor communications but to radio LAN for computers and other indoor communications as well.

This type of optoelectronic communication presents a need for transmitters, receivers, receiving optics, light modulators that are capable of high frequency modulation that are also compact in design and driven by low electric power.

This paper concerns a light modulator for converting electric signals from radio signals to optical signals. Various types of light modulators have been proposed. Some of them are based on direct modulation of LD while other external modulators are based on electric field absorption effect or electro-optic effect. Among them, the  $\text{LiNbO}_3$  (LN) light modulator based on electro-optic effect has been in use as a key element in long-distance digital communication because of low chirping in a broad-band application. This modulator requires a broad frequency band from the DC components, and contains a progressive wave electrode to meet this requirement. The modulating efficiency of this electrode configuration decreases at higher frequencies due to the speed matching between electricity and light, etc. For this reason, a high driving voltage is required to use the modulator in millimeter wave or higher frequencies.

On the other hand, optoelectronic communication needs a frequency response of only several GHz from the carrier frequency. This calls for a modulator that operates at a low driving voltage rather than the frequency bandwidth. Modulators with resonant electrodes have been proposed in this regard.<sup>5), 6)</sup> We have been doing basic studies on resonant type modulators with the carrier frequencies of 30GHz and 60GHz. Reported below is the result of prototyping and evaluation of such modulators in the 60GHz

band.

The study being reported below is a joint study by Optoelectronics Research Group, New Technology Research Laboratory of Sumitomo Osaka Cement Co., Ltd., and Communications Research Laboratory, Ministry of Posts and Telecommunications.

## 2. Operating Principle

The modulator consists of an optical waveguide of the Mach-Zehnder design and a modulating electrode. Light reaching the modulator is intensity-modulated by the electrode before it is emitted. Fig. 1 (a) shows the element configuration of the modulator.

The electrode consists of a feeding line, a resonant line, and an impedance matching element. The resonant line consists of an open-ended line of a finite length, and the line length is a key design element because of the three requirements mentioned below.

- a) Resonance must occur at the desired frequency in the resonant line.
- b) Impedances must match between the resonant line and the feeder line to ensure efficient application of input signals to the resonant line.

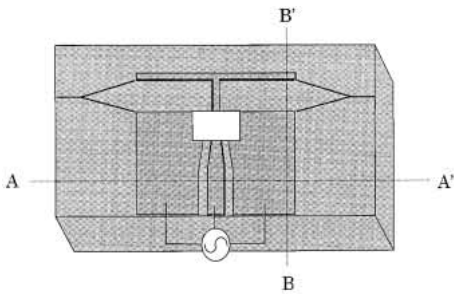


Fig. 1(a) Resonant modulator model

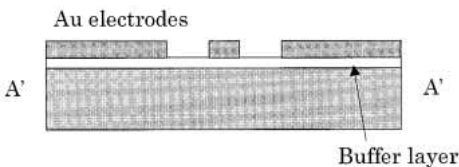


Fig. 1(b) Cross section A-A

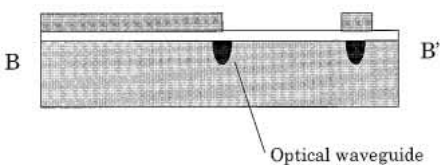


Fig. 1(c) Cross section B-B

- c) The amount of optical phase change due to electric signals must be large.

These three requirements are explained in more detail below starting with requirements a) and b).

The feeder line consists of coplanar lines with  $50\Omega$  impedance for matching with transmitters and

The resonant line of a finite length is connected to the feeder line in such a way the signal is reflected at line ends to produce amplitude higher than the input voltage amplitude, so that a high modulation efficiency can be

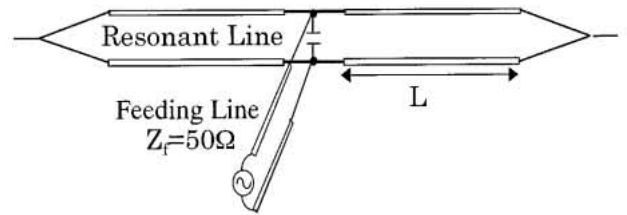


Fig. 2 Equivalent circuit model

achieved. Fig. 2 shows an approximate TEM equivalent circuit model.

Assume impedances of the feeder line and the resonant line to be  $Z_f$  and  $Z_r$ , respectively, and the propagation constant of the resonant line to be  $\gamma (= \alpha + j\beta)$ . Then, the standard admittance ( $Y_e$ ) of the resonant line standardized to the feeder line may be expressed as following:

$$Y_e = 2 \frac{Z_f}{Z_r} \tan \gamma L = g_e + j b_e \quad \dots (1)$$

Since the propagation constant  $\gamma$  is determined by the frequency and the line design, it may be considered a constant. Now, a capacity element is inserted between the feeder line and the resonant line while considering impedance matching between them. Assuming the standardized susceptance of the capacity element to be  $b_c$ , the standardized admittance ( $Y_N$ ) as seen from the feeder line can be expressed as following:

$$Y_N = Y_e + j b_c = g_e + j(b_e + b_c) \quad \dots (2)$$

$b_c$  will take a positive value since the capacity element is inserted in parallel to the resonant line. Therefore, the electrode length  $L$  is selected in such a way  $g_e = 1$  and  $b_c$  is a negative value so that impedances will match between the feeder line and the resonant line.

Requirement c), the amount of optical phase change due to electric signals, is explained next.

Assuming the waveguide extends in the direction of axis-z and that the feed point is represented by z=0 and, further, that a modulation signal  $E_0 \cos(\omega(t-t_0))$  is entered to the feed point, the electric field standing wave on the line may be expressed as following:

$$E(z,t) = \text{Re} \left\{ E_0 T \frac{\cosh[\gamma(L-|z|)]}{\cosh(\gamma L)} e^{j\omega(t-t_0)} \right\} \dots (3)$$

where, T represents a voltage transmission coefficient at the feed point. Assuming the refractive index of the waveguide to be  $n_o$ , the electric field felt by light being guided can be expressed as following:

$$E(z, \frac{z}{c} n_o + t)$$

Further, the difference in the amount of phase change between the waveguides,  $\theta$  can be expressed as following:

$$\begin{aligned} \Delta\phi(t) &= \frac{\pi}{\lambda} n_o^3 r_{33} \Gamma_{21} \int_{-L}^L E(z, \frac{z}{c} n_o + t) dz \\ &= \frac{\pi}{\lambda} n_o^3 r_{33} \Gamma_{21} \cdot 2L \frac{V_0}{s} j(\omega) \cos(\omega t + \theta) \dots (4) \end{aligned}$$

where,  $\lambda$  represents the light wavelength,  $\Gamma_{21}$  is the coupling coefficient of the electric field and light,  $r_3$  is an electro-optic constant of LN,  $V_0$  is the voltage amplitude of the modulation signal, and  $\Psi(\omega)$  is the modulation factor.

While the electrode length L is limited by two other requirements a) and b), it can take one of several values. The amount of phase change  $\theta$  increases when the electrode length L is increased, but the change is only minimal due to the speed matching between the electric signal and light, etc. Consequently, the electrode length L is determined based on the amount of phase change based on design needs.

### 3. Evaluation Method

The modulator fabricated in the course of this study was evaluated at the driving voltage (half-wave voltage  $B\pi$ ). The method of calculating  $B\pi$  is explained below. Fig. 3 shows a schematic drawing of the light waveguides.

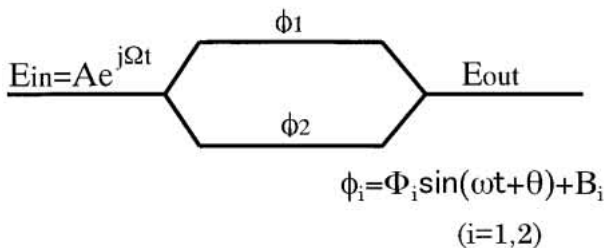


Fig. 3 Schematic drawing of the waveguides

The incident light  $E_{in}$ , branched at branch-Y, is subjected to phase changes  $\Phi_1$  and  $\Phi_2$ , respectively, when they travel through the waveguides and merged before being emitted as  $E_{out}$ , which can be expressed as the sum of Bessel functions as following:

$$\begin{aligned} E_{out} &= \frac{A}{2} [J_0(\Phi_1) e^{jB_1} + J_0(\Phi_2) e^{jB_2}] e^{j\omega t} \\ &+ \frac{A}{2} [J_1(\Phi_1) e^{jB_1} + J_1(\Phi_2) e^{jB_2}] e^{j(\omega + \omega) t} \\ &+ \dots \dots (5) \end{aligned}$$

Assuming  $P_{main}$  represents the light intensity of the incident light component (the term  $e^{j\omega t}$  in the above expression) and  $P_{side}$  represents the light intensity of the modulation signal component, they may be expressed as following:

$$P_{main} = \frac{|A|^2}{4} \cdot |J_0(\Phi_1) + J_0(\Phi_2) e^{j(B_2 - B_1)}|^2 \dots (6)$$

$$P_{side} = \frac{|A|^2}{4} \cdot |J_1(\Phi_1) + J_1(\Phi_2) e^{j(B_2 - B_1)}|^2 \dots (7)$$

Since these light intensities can be measured using an optical spectrum analyzer,  $P_{side}/P_{main}$  can be determined from the measured light intensities and then applied to the above expressions to determine phase changes  $\Phi_1$  and  $\Phi_2$ . Finally, the voltage, where the amount of phase change  $\Delta\phi$  ( $=|\Phi_2 - \Phi_1|$ ) equals to  $\pi$  from the relationship between  $\Delta\phi$  and the applied voltage  $V_0$  in the expression (4) above, is estimated to be half-wave voltage  $V\pi$ .

### 4. Production Parameters

Light waveguides are created by thermal diffusion of Ti on the Z-cut LN substrate, on which  $\text{SiO}_2$  is laminated as a  $0.55\mu\text{m}$  buffer layer. An electrode,  $1\mu\text{m}$  thick, is formed over the buffer layer.

A capacity element for impedance matching is provided by forming a film dielectric ( $\text{SiO}_2$ ) over the electrode and an electrode is constructed over the film to form a batch type capacitance.

The prototype was tested for operation at the central frequency of 60GHz. For the test purpose, the electrode length of 1.2mm was chosen based on the parameters in Table 1 and in such a way the requirements in Section 2 were met.

Table 1 Design parameters

Frequency (GHz)	60
Dielectric loss ( $\text{cm}^{-1}$ )	0.138
Conductor loss ( $\text{cm}^{-1}$ )	0.216
Microwave effective index of refraction	3.37

## 5. Methods and Results of Measurement

Fig. 4 shows the measurement setup in which the modulation signal is measured in one of the two methods: The modulation signal is received by a photo diode (PD) and the actual waveform (time waveform) is measured with a digital oscilloscope; or measured with an optical spectrum analyzer.

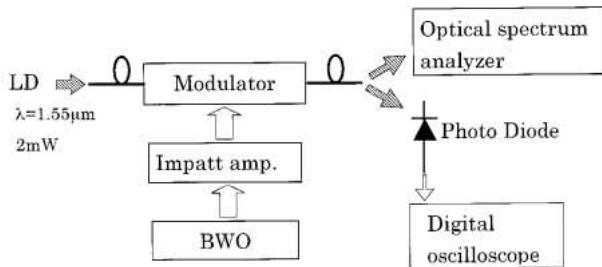


Fig. 4 Measurement setup

Fig. 5 shows the observation of the actual waveform measured with the optical output connected to the PD. A modulation signal at 57.4GHz was identified.

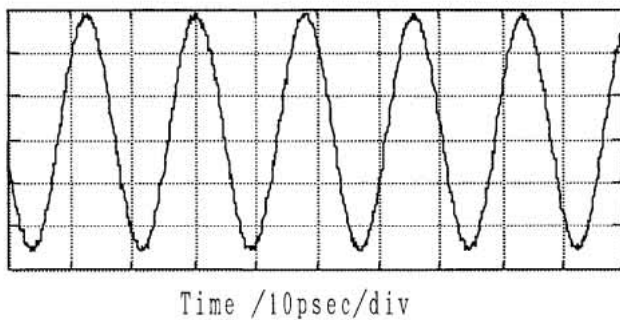


Fig. 5 Observed waveform of modulated light signal

Fig. 6 shows the results of observation by an optical spectrum analyzer. Fig. 6(a) shows the result without the modulation signal. The LD wavelength characteristics are observed. Fig. 6(b) shows the result with the modulation signal applied to the modulator. The modulation signal frequency is 57.4GHz. Sidebands can be seen next to the LD wavelength, indicating that the modulation was successful.

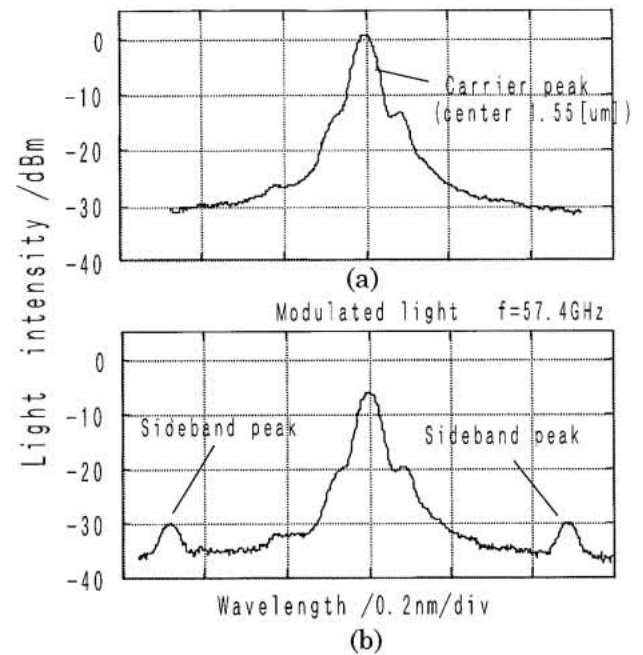


Fig. 6 Optical spectrum of modulated light

The measurement results were analyzed by the methods explained in Section 3 above. The half-wave voltage was estimated to be approximately 14V, and the product of the half-wave voltage and the electrode length  $V\pi \cdot 2L$  to be 3.3V.cm.

Fig. 7 shows the measured and theoretical values of frequency dependence of the modulation factor  $\Psi(\omega)$ . This suggests the 3dB modulation band to be around 1GHz. The designed central frequency of 60GHz turned out to be 57.4GHz, likely due to the deviations of the designed electrode loss and effective index of refraction of the electric signal.

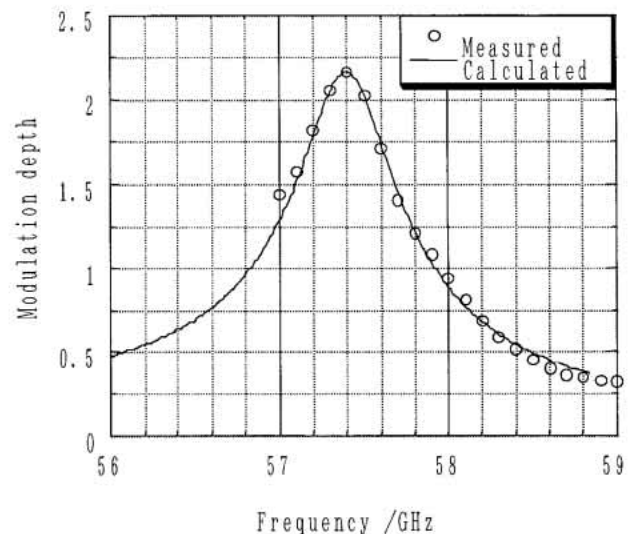


Fig. 7 Frequency dependence of the modulation factor

## 6. Conclusions

A 60GHz band resonant modulator was designed and prototyped with the electrode length of  $L=1.2\text{mm}$ . It yielded a half-wave voltage of  $V\pi=14\text{V}$ , and a modulation index of  $V\pi\cdot 2L=3.3\text{V}\cdot\text{cm}$  at the central frequency of 57.4GHz. In comparison with a progressive wave type modulator with the electrode length of about 40mm, the  $V\pi$  was nearly the same but the  $V\pi\cdot 2L$  showed some improvement because of the shorter electrode length. This suggests that the prototype represents a modulator of high efficiency. Continued efforts will be made to reduce the  $V\pi$  value by means of optimizing the electrode design such as a modified electrode structure, using tiered electrodes, etc. In addition to the 60GHz band application, similar studies are planned for the 30GHz band for which a high demand is expected.

## 7. Acknowledgement

This paper is a result of a joint study by Optoelectronics Research Group, New Technology Research Laboratory of Sumitomo Osaka Cement Co., Ltd., and Communications Research Laboratory, Ministry of Posts and Telecommunications. We thank the members of Optoelectronics Research Group and Optical Information Processing Research Room of Optical Engineering Dept., of Communications Research Laboratory for their cooperation.

## References

- 1) Izutsu, *Transactions of IEICE*, C-1 Vol. J81-C-1, No. 2, pp. 47-54.
- 2) IEICE Trans. On Comm., Vol. E76-B, No. 9, Sept., 1993.
- 3) Tsukamoto and Otsuka, *Journal of IEICE*, Vol. 80, No. 8, pp. 859-868, Aug. 1998.
- 4) S. Komaki, K. Tsukamoto, and M. Okada, *IEEE Trans. Microwave Theory Tech*, Vol. 43, pp. 2222-2228, Sept., 1995.
- 5) Izutsu, Murakami, and Sueda, *Transactions of IEICE*, C. Vol. J71-C, No. 5, pp. 653-658, 1988.